Anisotropic Power Law Strain Correlations in Sheared Amorphous 2D Solids

C. E. Maloney[1,2] and M. O. Robbins[2]

[1]*Department of Civil and Environmental Engineering, Carnegie Mellon University, Pittsburgh, Pennsylvania 15213, USA*
[2]*Department of Physics and Astronomy, Johns Hopkins University, Baltimore, Maryland 21218, USA*

The local deformation of steadily sheared two-dimensional Lennard-Jones glasses is studied via computer simulations at zero temperature. In the quasistatic limit, spatial correlations in the incremental strain field are highly anisotropic. The data show power law behavior with a strong angular dependence of the scaling exponent, and the strongest correlations along the directions of maximal shear stress. These results support the notion that the jamming transition at the onset of flow is critical, but suggest unusual critical behavior. The predicted behavior is testable through experiments on sheared amorphous materials such as bubble rafts, foams, emulsions, granular packings, and other systems where particle displacements can be tracked.

The microscopic mechanisms underlying shear deformation in amorphous systems are of great technological importance [1,2]. A wide range of experimental systems exhibit similar behavior, including granular materials, metallic glasses, foams, colloids, and emulsions. These systems have also been the focus of increasing fundamental interest due to unifying theoretical concepts such as jamming [3], shear transformation zones [4,5], dynamical heterogeneity [6], and effective temperature [7].

In this Letter we examine spatial correlations in the plastic deformation produced by slowly shearing an amorphous system at zero temperature. We consider the quasistatic limit of a system with underdamped dynamics, rather than minimizing energy as in previous work [2,8]. An unconventional measure of shear reveals correlations in both the magnitude and direction of shear. Using systems 3 orders of magnitude larger than in previous studies of similar systems [8,9] allows angle-resolved spatial correlations to be measured over more than a decade in wave vector.

The results suggest that zero-temperature sheared amorphous systems belong to a class of systems that exhibit critical behavior when driven slowly, such as model sandpiles [10], disordered ferromagnets [11], rupturing faults [12], and plastically deformed crystals [13]. However, the correlations in sheared amorphous systems have a novel form. Strain correlations decay as a power of wave vector with strong angular anisotropy in both the exponent and prefactor. These correlations may have important implications for theories of plasticity in amorphous materials [4,5,14]. While we present results for a binary Lennard-Jones mixture under pure shear, tests with other interaction potentials and simulation protocols show consistent behavior.

We consider a bidisperse mixture of particles that is chosen to inhibit crystallization [8]. There are N_L large (L) particles and N_S small (S) particles with $N_L/N_S =$ $(1 + \sqrt{5})/4$. Particles of type I and J interact with a Lennard-Jones potential: $U_{IJ} = 4\epsilon[(r/\sigma_{IJ})^{-6} - (r/\sigma_{IJ})^{-12}]$, where ϵ and σ_{IJ} set the characteristic strength and range of the interaction and r is the particle separation. To speed calculations the interaction is truncated smoothly between $r_{in} = 1.2\sigma_{IJ}$ and $r_{out} = 1.5\sigma_{IJ}$ using a fourth-order polynomial [15]. We set $\sigma_{LL} = 1.0\sigma_0$, $\sigma_{SS} = 0.6\sigma_0$, and $\sigma_{LS} = 0.5(\sigma_{LL} + \sigma_{SS}) = 0.8\sigma_0$ and measure all lengths in units of σ_0. The characteristic time $\tau \equiv \sqrt{m\sigma_0^2/\epsilon}$, where m is the mass of all particles.

The equations of motion are integrated with LAMMPS [15] using the velocity-Verlet algorithm and a time step of 0.0056τ. Periodic boundary conditions are used with periods L_x and L_y. Amorphous states are prepared as in Ref. [8], and the steady state behavior considered here is insensitive to the equilibration procedure. The system is maintained at zero temperature by a Galilean-invariant Kelvin damping force equal to the relative velocity between interacting particles times a damping constant $\Gamma = 0.45m/\tau$. For this Γ, vibrations of wavelength larger than the interparticle spacing are underdamped. The limit of zero temperature is relevant for systems where particles represent grains or colloids and is of fundamental interest as a limiting case for atomic systems.

Systems are compressed along the y direction at constant true strain rate $\dot{\gamma}$ and expanded along x to maintain constant area. Results are presented for an ensemble of four systems with initial periods $L_{x0} \approx L_{y0} \approx 1000\sigma_0$, $N_L + N_S \approx 1.6 \times 10^6$, and $\dot{\gamma} = 0.45 \times 10^{-5}$. Consistent results were obtained for systems with $\dot{\gamma}$ and L varied by an order of magnitude and for simple shear of systems between rough walls. The incremental plastic strain is examined over strain intervals $\Delta\gamma \gtrsim 0.001$ that are long enough for stress to equilibrate across the sample via sound propagation. Studies of different system sizes and rates showed that for these conditions the system is in the quasistatic limit

where the accumulated plastic strain depends only on $\Delta\gamma$ rather than on the time interval and rate separately. As γ increases from zero, there is a slow rise in the stress, and changes are observed in other statistical quantities. For $\gamma > 0.06$ the system appears to be in steady state. The results presented below are averaged over γ between 12% and 24%.

In continuum mechanics, strain is defined in terms of derivatives of the displacement field. A finite-difference scheme must be used to obtain the strain in our discrete system. The Delaunnay triangulation of an initial configuration is computed. A constant displacement gradient tensor within each triangle is then defined from a linear fit to the differential displacements **u** of the three vertices over a small $\Delta\gamma$. Fourier transforms were obtained by sampling on a fine, rectangular grid.

In 2D, the displacement field is determined up to a constant by its divergence, $\phi = \partial_x u_x + \partial_y u_y$, and curl, $\omega = \partial_y u_x - \partial_x u_y$. The former gives information about local dilation, while the latter gives information about shear. Changes in ϕ are typically at least an order of magnitude smaller than ω, because density changes produce a larger increase in energy than shear does. We focus on ω which provides information about both the magnitude and direction of shear. Positive values indicate shear with clockwise vorticity and $\omega < 0$ implies counterclockwise vorticity.

Figure 1 shows a typical ω field for a strain increment of $\Delta\gamma = 0.004$. Long-range, highly anisotropic correlations are evident. There are elongated regions of clockwise slip along the downward diagonal and regions of counterclockw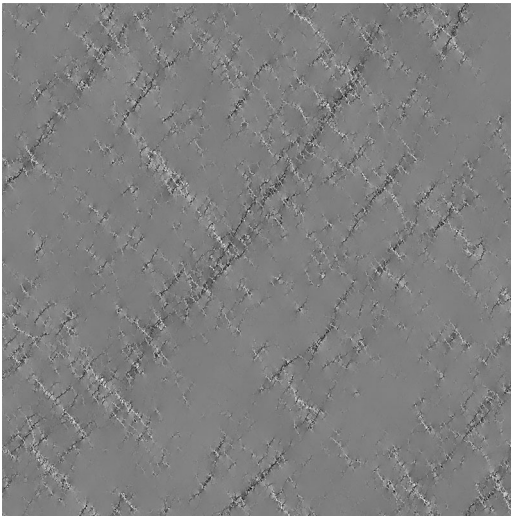ise slip along the upwards diagonal [16]. The contrast between these two conjugate systems is completely missed by conventional measures of shear strain that are not sensitive to the sense of rotation.

To quantify the angle-dependent correlations we calculate the power spectrum, $S(\mathbf{q}) \equiv \langle |\omega(\mathbf{q})|^2 \rangle$, where $\omega(\mathbf{q})$ is the Fourier transform of the vorticity, $\mathbf{q}$ is the wave vector, and angle brackets indicate an average over many intervals of the same $\Delta\gamma$ in four different systems. To further reduce noise, results were averaged over angular bins of width $\pi/64$ and 20 evenly spaced intervals in $\ln q$. The maximum q considered, $q = \pi/\sigma_0$, corresponds to a wavelength of two particle diameters. As q decreases, the number of discrete wave vectors in a given range of $\ln q$ decreases, increasing statistical noise and decreasing the achievable resolution in angle θ relative to the x axis. For this reason we focus on $q > 2\pi/100\sigma_0$, corresponding to wavelengths of $1/10$ the system size or less.

We first illustrate that the scaling of $S(q, \theta)$ with q is relatively insensitive to $\Delta\gamma$. The average of $\log_{10} S$ over all angles is plotted against $\log_{10} q$ in Fig. 2(a) for different $\Delta\gamma$. S increases nearly linearly with $\Delta\gamma$ for all q, which implies that strains from successive intervals add incoherently. This is confirmed by direct evaluation of two-time cross correlation functions. Figure 2(b) shows the apparent scaling exponent, $\langle\alpha\rangle \equiv -\partial\langle\ln S\rangle/\partial\ln q$. Because the correlation functions for different $\Delta\gamma$ are scaled by q-independent factors, the results for $\langle\alpha\rangle$ collapse on a single curve. Over an intermediate range of q the apparent angle-averaged exponent is 0.68 ± 0.02. However, as we now show, the scaling exponent is strongly dependent on θ.

Figure 3(a) shows log-log plots of $S(q, \theta)$ vs q at five values of θ for $\Delta\gamma = 0.001$. Only angles between 0 and $\pi/2$ are shown because of symmetry. $S(q, \theta)$ has inversion
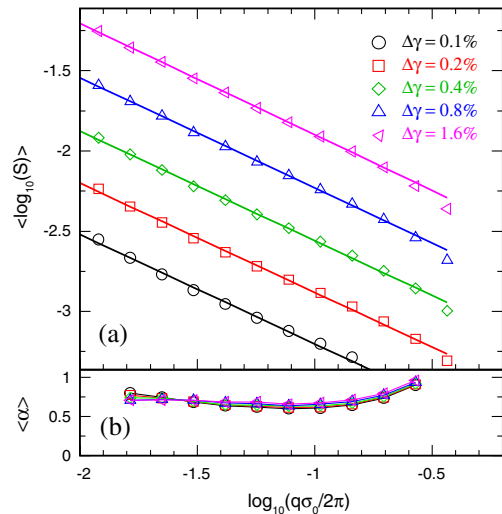

FIG. 1. Gray scale image of $\omega \equiv \partial_y u_x - \partial_x u_y$ from a typical strain interval, $\Delta\gamma = .004$, in steady state. The system is compressed along the vertical y axis and expands along the horizontal x axis to maintain constant area. The gray scale is linear and ranges from -0.2 (black) to $+0.2$ (white), and the image is rendered in the initial (square) reference frame.

FIG. 2 (color online). (a) The angle average $\langle\log_{10} S\rangle$ as a function of $\log_{10} q$ for the indicated $\Delta\gamma$. Straight lines are best fits which all yield the same slope -0.68 ± 0.02. (b) Apparent exponent $\langle\alpha\rangle \equiv -\Delta\langle\ln S\rangle/\Delta\ln q$ as a function of $\log_{10} q$ calculated from a centered finite difference.
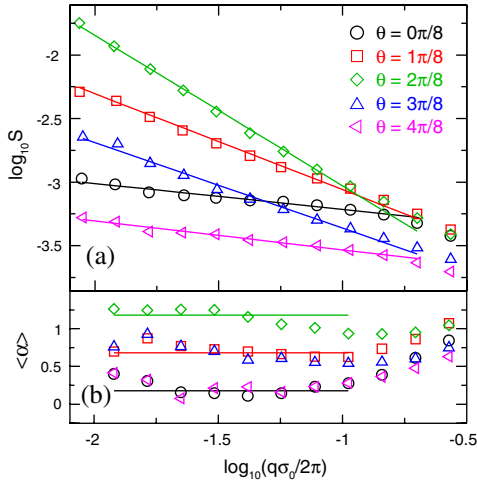
FIG. 3 (color online). (a) Variation of $\log_{10}S(q, \theta)$ with $\log_{10}(q)$ at $\Delta\gamma = 0.001$. The five different data sets correspond to angular wedges of width $\pi/64$ centered at $\theta = n\pi/8$ and lines show linear fits. Variations between samples are comparable to the symbol size. (b) Apparent exponent $\alpha(q, \theta) \equiv -\Delta \ln S(q, \theta)/\Delta \ln q$ for the same set of angles evaluated using a centered finite difference. Lines correspond to $\alpha(\theta) = 0.68 - 0.5 \cos(4\theta)$.

symmetry ($\theta \leftrightarrow \theta + \pi$) by construction. The statistical average also has symmetry about the principal axes, although individual ω fields can strongly violate this symmetry, favoring *either* positive vorticity organized along $-\pi/4$ *or* negative vorticity organized along $+\pi/4$.

For each orientation S decays as a power of q over about a decade. Both the prefactor S_0 and exponent α describing the decay are angle dependent:

$$S(q, \theta) = S_0(\theta)q^{-\alpha(\theta)}. \qquad (1)$$

Figure 3(b) shows the effective exponent, $\alpha(\theta) \equiv -\partial \ln S/\partial \ln q$, for each θ. The exponent changes by about a factor of 5 with θ, while fluctuations with q are comparable to statistical and systematic uncertainties. Note that because of this strong variation with θ, the lines in Fig. 2 would not be straight if we had performed the angle average before taking the logarithm of S.

As expected from Fig. 1, the correlations and scaling exponent are largest for $\theta = \pi/4$ [16]. The scaling exponent appears to be symmetric about $\theta = \pi/4$, and results for all θ are well fit by $\alpha(\theta) = 0.68 - 0.5 \cos(4\theta)$. The prefactor does not have the same symmetry. For the examples shown, the prefactor is larger for $\theta = \pi/8$ than $3\pi/8$ and for $\theta = 0$ than $\pi/2$. The same trend is seen for other θ. To help explain the angle dependence of the prefactor and exponent, we now consider the shear and normal forces on planes with different orientations.

The stress tensor is approximately diagonal throughout the simulation, implying that the principal axes remain close to x and y. Two invariants can be constructed from the eigenvalues λ_i of the stress tensor. One is the pressure $p = -(\lambda_x + \lambda_y)/2$ and the other a measure of shear stress $s = (\lambda_x - \lambda_y)/2$, where $\lambda_x > \lambda_y$ since compressive stresses are negative. The normal N and tangential T stresses on a plane whose normal is at an angle θ relative to the x axis can be found by transforming the stress tensor: $N = p - s\cos(2\theta)$ and $T = s\sin(2\theta)$. Note that T is symmetric about $\theta = \pm\pi/4$ while N is not.

The magnitude of the tangential stress is largest for $\theta = \pm\pi/4$. The sign of T favors clockwise slip for $\theta = \pi/4$ and counterclockwise slip along $\theta = -\pi/4$, as observed in Fig. 1. Aligning plastically sheared regions of each sense along the corresponding directions is the most efficient way of releasing the elastic energy built up by compression along the y axis.

While this explains why correlations along $\pm\pi/4$ are largest at small q (large scales), it neglects barriers to the initiation of plastic deformation. The Mohr-Coulomb model assumes that the stress needed to initiate plastic shear increases with normal load, much like friction forces between macroscopic objects. Shear should then occur on planes where $|T/N|$ is largest. Decreasing $|\theta|$ from $\pi/4$ produces a linear decrease in N, while T only decreases quadratically from its maximum value. Thus the Mohr-Coulomb model predicts the normal to the shear plane should be tilted to smaller θ (away from the compressive axis). As expected from this argument, the peak in $S(q)$ is shifted to $\theta < \pi/4$ at large q (small distances). This shift only appears in the prefactor S_0 and not in the scaling exponent α. Thus the asymmetry about $\pm\pi/4$ decreases with decreasing q (increasing distance) and there is no unique shear orientation as usually assumed in Mohr-Coulomb treatments.

Elastic interactions have a power law character and one might wonder if simple arguments based on elastic interactions could explain the observed exponents. Consider first the linear elastic response of the entire amorphous system to a small strain [17–19]. Leonforte and co-workers [20] found that the amplitude of the projection of the *elastic* displacement fields onto transverse (and longitudinal) plane waves is proportional to $1/q$. This implies that the Fourier transforms of ω (and ϕ) are independent of q, corresponding to $\alpha = 0$. Alternatively, one might imagine that the correlations come from the incoherent sum of elastic quadrupoles generated by localized plastic shear zones [8]. In 2D, this generates an ω field which has a quadrupolar prefactor, but is again q independent at small q. No simple elastic mechanism yields the long-range, anisotropic correlations that we observe.

Power law correlations in incremental plastic displacements under slow shear have been reported for a granular model that included frictional forces between particles [21]. The system was subjected to simple shear and correlations in the longitudinal and transverse incremental displacement decayed as $q^{-1.25}$ along the imposed flow

direction. This orientation would correspond to $\theta = \pm\pi/4$ in our geometry, but the similarity in exponents appears coincidental. Since ω represents a derivative of the incremental displacement, $S(q)$ should contain an extra factor of q^2. The results of Radjai and Roux for displacement would thus imply $\alpha = -0.75$, which is qualitatively inconsistent with our result. The much smaller system sizes used in Ref. [21] prevented studies of scaling in other orientations, and it would be interesting to revisit this system to determine which microscopic parameters (particle-level friction, viscous damping mechanisms, etc.) affect the emergent scaling behavior.

The novel anisotropic scaling behavior observed in the atomistic model studied here should serve as a benchmark for coarse-grained models of plasticity. Early theories of plasticity in amorphous materials were mean field models [4,14]. More recent theories incorporate spatial variation [5], leading to spatially extended, anisotropic failure that may be related to the strain correlations observed here. Two lattice models have also been developed that include redistribution of stress after a local yield event [22], but we are not aware of any study of spatial correlations in the resulting plastic displacements. Baret and co-workers [23] developed a stochastic lattice model for a system sheared along z and with the displacement gradient along y. The system is quasi-2D, with the shear displacement $h(x, y)$ independent of z. While this is a very different geometry than ours, it is interesting to note that h scaled with different power laws along the neutral x and strain gradient y directions. Unfortunately, no observations were made for wave vectors at intermediate orientations.

In conclusion, the results presented here provide evidence for novel critical scaling behavior in the quasistatic limit of dynamically sheared amorphous systems. Analyzing both the magnitude and direction of shear strain reveals rich spatial structure and an unusual angle-dependent scaling exponent with fourfold symmetry. The lower symmetry of the scaling prefactor S_0 can be understood from a Mohr-Coulomb model for initiation of plastic yield. The resulting asymmetry in $S(q)$ decreases with increasing length scale (decreasing q).

Similar behavior should be observed in 2D granular systems, foams, colloids, and other disordered, athermal systems. The analysis used here is readily applied to laboratory experiments on these systems using existing particle tracking techniques. Interesting questions for future studies will be the role of dimensionality and whether thermal fluctuations change the scaling behavior of displacements in sheared systems.

[1] A. Argon, Acta Metall. **27**, 47 (1979); K. Maeda and S. Takeuchi, Philos. Mag. A **44**, 643 (1981).

[2] D. Srolovitz, V. Vitek, and T. Egami, Acta Metall. **31**, 335 (1983).

[3] A. Liu and S. Nagel, Nature (London) **396**, 21 (1998).

[4] M. L. Falk and J. S. Langer, Phys. Rev. E **57**, 7192 (1998); M. L. Falk, J. S. Langer, and L. Pechenik, Phys. Rev. E **70**, 011507 (2004).

[5] M. L. Manning, J. S. Langer, and J. M. Carlson, Phys. Rev. E **76**, 056106 (2007); M. L. Manning, E. G. Daub, J. S. Langer, and J. M. Carlson, Phys. Rev. E **79**, 016110 (2009).

[6] W. Kob, C. Donati, S. Plimpton, P. Poole, and S. Glotzer, Phys. Rev. Lett. **79**, 2827 (1997); C. Donati, J. Douglas, W. Kob, S. Plimpton, P. Poole, and S. Glotzer, Phys. Rev. Lett. **80**, 2338 (1998); E. Weeks, J. Crocker, A. Levitt, A. Schofield, and D. Weitz, Science **287**, 627 (2000);

[7] L. Cugliandolo and J. Kurchan, Phys. Rev. Lett. **71**, 173 (1993); I. Ono, C. O'Hern, D. Durian, S. Langer, A. Liu, and S. Nagel, Phys. Rev. Lett. **89**, 095703 (2002); L. Berthier and J. Barrat, Phys. Rev. Lett. **89**, 095702 (2002).

[8] C. Maloney and A. Lemaitre, Phys. Rev. Lett. **93**, 016001 (2004); Phys. Rev. E **74**, 016118 (2006).

[9] A. Tanguy, F. Leonforte, and J. L. Barrat, Eur. Phys. J. E **20**, 355 (2006).

[10] P. Bak, C. Tang, and K. Wiesenfeld, Phys. Rev. Lett. **59**, 381 (1987).

[11] H. Ji and M. O. Robbins, Phys. Rev. B **46**, 14519 (1992); O. Perkovic, K. Dahmen, and J. Sethna, Phys. Rev. Lett. **75**, 4528 (1995).

[12] J. Carlson, J. Langer, and B. Shaw, Rev. Mod. Phys. **66**, 657 (1994).

[13] M.-C. Miguel, A. Vespignani, S. Zapperi, J. Weiss, and J. Grasso, Nature (London) **410**, 667 (2001); M. Koslowski, R. LeSar, and R. Thomson, Phys. Rev. Lett. **93**, 125502 (2004).

[14] P. Sollich, F. Lequeux, P. Hebraud, and M. E. Cates, Phys. Rev. Lett. **78**, 2020 (1997).

[15] S. J. Plimpton, J. Comput. Phys. **117**, 1 (1995); http://www.cs.sandia.gov/sjplimp/lammps.html.

[16] Correlations occur along $\pm\pi/4$ even when the ratio L_x/L_y is changed from unity.

[17] A. Tanguy, J. Wittmer, F. Leonforte, and J. Barrat, Phys. Rev. B **66**, 174205 (2002).

[18] B. A. DiDonna and T. C. Lubensky, Phys. Rev. E **72**, 066619 (2005).

[19] C. E. Maloney, Phys. Rev. Lett. **97**, 035503 (2006).

[20] F. Leonforte, R. Boissiere, A. Tanguy, J. Wittmer, and J. Barrat, Phys. Rev. B **72**, 224206 (2005).

[21] F. Radjai and S. Roux, Phys. Rev. Lett. **89**, 064302 (2002).

[22] V. Bulatov and A. Argon, Model. Simul. Mater. Sci. Eng. **2**, 203 (1994); G. Picard, A. Ajdari, F. Lequeux, and L. Bocquet, Phys. Rev. E **71**, 010501 (2005).

[23] J. Baret, D. Vandembroucq, and S. Roux, Phys. Rev. Lett. **89**, 195506 (2002).